Diffusion Barriers Evoked in the Rat Cortex by Reactive Astrogliosis

TAMARA ROITBAK AND EVA SYKOVÁ*
*Department of Neuroscience, 2nd Medical Faculty, Charles University
and Institute of Experimental Medicine AS CR, Prague, Czech Republic*

ABSTRACT   Changes in extracellular space (ECS) diffusion parameters in astrogliotic tissue around a unilateral cortical stab wound were determined from concentration-time profiles of tetramethylammonium (TMA^+) using TMA^+-selective microelectrodes. Three diffusion parameters—ECS volume fraction α (α = ECS volume/ total tissue volume), tortuosity λ ($\lambda^2 = D/ADC$; where D is the free and ADC is the apparent diffusion coefficient of TMA^+ in the brain), and nonspecific TMA^+ uptake k'—were determined at 3, 7, 21, and 35 days postwounding (dpw), in the hemispheres ipsilateral and contralateral to the lesion. Following diffusion experiments, tissue sections were immunostained for glial fibrillary acidic protein (GFAP) and chondroitin-sulphate proteoglycans (CSPG). In the area 300–1000 µm around the wound, α was increased at 3, 7, and 21 dpw by about 20% but returned to control values at 35 dpw; λ was increased at all four intervals, reaching a maximum at 7 dpw. k' was lower than in the contralateral hemisphere at 7, 21, and 35 dpw. Measurements 1,500–2,000 µm from the wound revealed only an increase in λ at 7 dpw. The time course of changes in ECS diffusion parameters closely correlated with increased staining for GFAP and CSPG. Our results show that astrogliosis significantly changes the diffusion properties of nervous tissue, making it less permissive. Both hypertrophied astrocytic processes and an enhanced formation of some extracellular matrix molecules could affect, through changes in the diffusion of molecules in the ECS, neuron–glia communication, "cross-talk" between synapses, extrasynaptic transmission, and regenerative processes. *GLIA 28:40–48, 1999.*
© 1999 Wiley-Liss, Inc.

INTRODUCTION

Numerous studies have shown reactive gliosis to be a common phenomenon in the CNS following different neurological disorders and brain trauma (Bignami and Dahl, 1974; 1995; Nathaniel and Nathaniel, 1981; Lindsay, 1986; Hozumi et al., 1990; Hatten et al., 1991). This reaction of glial cells is characterised by astrocyte proliferation; extensive hypertrophy of nuclei, cell bodies, and processes; and increased expression of the astrocyte marker glial fibrillary acidic protein (GFAP). The hypertrophied processes of "reactive astrocytes" fill the space resulting from a loss of myelin and neurons and, in most cases, form a glial scar. Reactive gliosis is a complex phenomenon leading to either neuronal survival or death and axonal regeneration or retraction. In certain conditions, reactive astrocytes may provide a permissive substratum to support axonal regrowth; in others the scar is a nonpermissive substratum (for review see Ridet et al., 1997). It is not clear whether or how reactive astrocytes and astrogliosis, a characteristic response of astrocytes to injury in numerous pathological states such as chronic ischemia, excessive excitation (e.g., epileptic seizures), Alzheimer's disease, degeneration during AIDS encephalopathy, and multiple sclerosis, change the extracellular space (ECS) volume and its geometry in the injured nervous tissue.

A stab wound of the rodent brain is a well-characterized as well as the most common model of reactive gliosis (Norton et al., 1992). In this study we measured the ECS diffusion parameters in tissue surrounding a stab wound 3, 7, 21, and 35 days postwounding (dpw). Reactive astrogliosis could impose diffusion barriers in the CNS due to a hypertrophy of astrocytic processes and, presumably, due to an increased production of extracellular matrix components (Hatten et al., 1991; Ridet et al., 1997). Astrogliosis could therefore affect the movement of neuroactive substances in the ECS by diffusion, which is the underlying mechanism of glia–neuron communication, extrasynaptic transmission, and "cross-talk" between synapses (Fuxe and Agnati, 1991; Syková, 1992, 1997; Agnati et al., 1995; Bjelke et al., 1995; Kullmann and Asztely, 1998; Nicholson and Syková, 1998; Zoli et al., 1999).

The diffusion of substances released from neurons or glial cells to the ECS is hindered by three diffusion factors (Nicholson and Phillips, 1981). First, diffusion in the ECS is constrained by the restricted volume of the tissue available for diffusing particles, i.e., by the extracellular volume fraction α = ECS volume/total tissue volume. Second, tortuosity, λ ($\lambda^2 = D/ADC$, where D is the free diffusion coefficient and ADC is the apparent diffusion coefficient in the brain), represents the restrictions for diffusion in the ECS that are imposed by cellular membranes, neuronal and glial processes, fixed negative/positive surface charges, glycoproteins, and macromolecules of the extracellular matrix. Besides these two constraints, the diffusion of some substances may be affected by nonspecific uptake, k', a factor describing the loss of a substance across cell membranes.

MATERIALS AND METHODS
Animal Preparation

Adult male Wistar rats 2.5–3 months old (200–300 g) were anesthetized by an intraperitoneal injection of 60 mg/kg pentobarbital. Part of the skull was unilaterally removed with a dental drill, and a fine microdissecting knife was used to make a stab wound 4 mm long and 2 mm deep rostral from the lambda and 2 mm from the midline. The skin overlying the cranium was sutured.

At 3, 7, 21, or 35 days postwounding (dpw), the animals were used in diffusion experiments. The animals were anesthetized by an intraperitonial injection of pentobarbital (60 mg/kg), and a state of deep anesthesia was maintained throughout the experiment by injection of 15 mg/kg every 2–3 h. The brain surface above the wounded area was exposed by removing the cranial bones with a dental burr and forceps. A second opening was made above the cortical surface of the contralateral hemisphere at the same level. The dura matter was removed above both openings, and the head of the animal was fixed in a stereotaxic apparatus. Animals were warmed by a heating pad to maintain body temperature at 37°C. The exposed brain tissue was bathed in warm (37–38°C) artificial cerebrospinal fluid (Lehmenkühler et al., 1993). Electrodes were placed above the brain surface, and penetrations were performed using a remote control micromanipulator (Nanostepper; SPI, Oppenheim, Germany). The tracks were made either in the vicinity of the wound (300–1000 μm laterally from the wound) or at a distance of 1,500–2,000 μm. Diffusion curves were recorded from depths of 500 μm to 1,900 μm in 200 μm steps. Control measurements in the contralateral hemisphere of operated animals were made before and/or after the measurements at the wounded site. These data were also compared to measurements done on intact animals (Mazel et al., 1998).

Diffusion Measurements

TMA$^+$-selective microelectrodes were used to measure the diffusion properties of wounded and intact cerebral cortex. TMA$^+$-selective microelectrodes were made from double-barreled tubing as described elsewhere (Syková et al., 1994). The ion exchanger was Corning 477317, and the ion-sensing barrel was backfilled with 100 mM TMA chloride, whereas the reference barrel contained 150 mM NaCl. Electrodes were calibrated in a solution of 150 mM NaCl + 3 mM KCl with the addition of TMA$^+$ at the following concentrations (in mM): 0.01, 0.03, 0.1, 0.3, 1, 3, 10. Calibration data were fitted to the Nikolsky equation to determine electrode slope and interference. Iontophoresis pipettes were prepared from theta glass. The shank was bent before backfilling with 100 mM TMA chloride, so that it could be aligned parallel to that of the ISM. Electrode arrays were made by gluing together an iontophoresis pipette and a TMA$^+$-sensitive microelectrode with a tip separation of 120–180 μm. Iontophoresis parameters were a +20 nA bias current (continuously applied to maintain a constant electrode transport number) and a +80 nA current step of 60 s duration to generate TMA$^+$ diffusion curves. Potentials recorded at the reference barrel of the ISM were subtracted from the ion-selective barrel measurements by means of a buffer and subtraction amplifier. TMA$^+$ diffusion curves were captured on a digital oscilloscope (Nicolet 310), then transferred to a PC-compatible Pentium computer and analyzed by fitting the data to a solution of the diffusion equation by the use of the program VOLTORO (C. Nicholson, unpublished). TMA$^+$ concentration-vs.-time curves were first recorded in 0.3% agar gel (Difco Agar Noble) made up in 150 mM NaCl, 3 mM KCl and 1 mM TMA$^+$. The diffusion curves in agar were used to determine the electrode transport number, n, and free TMA$^+$ diffusion coefficient, D (cm^2 s^{-1}). Diffusion curves were then recorded in the brain and analyzed to yield a value of α, the TMA$^+$ apparent diffusion coefficient in tissue, ADC_{TMA} (cm^2 s^{-1}), λ and nonspecific TMA$^+$ uptake, k' (s^{-1}; Nicholson and Phillips, 1981; Nicholson and Syková, 1998). These parameters were extracted by a nonlinear curve-fitting simplex algorithm operating on

the diffusion curve described by equation 1, which represents the behavior of TMA$^+$, assuming that it spreads out with spherical symmetry, when the iontophoresis current is applied for duration S (Nicholson and Phillips, 1981). In this expression, C is the concentration of TMA$^+$ at time t and distance r. The equation governing diffusion in brain tissue is:

$$C = G(t) \qquad t < S \text{ for the rising phase}$$
$$\text{of the curve}$$
$$C = G(t) - G(t - S) \quad t > S \text{ for the falling phase}$$
$$\text{of the curve.}$$

The function $G(u)$ is evaluated by substituting t or $t - S$ for u in the following equation:

$$G(u) = (Q\lambda^2/8\pi D\alpha r)\{\exp[r\lambda(k'/D)^{1/2}]$$
$$\times \; erfc[r\lambda/2(Du)^{1/2} + (k'u)^{1/2}]$$
$$+ \exp\;[-r\lambda(k'/d)^{1/2}erfc[r\lambda/2(Du)^{1/2} - (k'u)^{1/2}]\} \quad (1)$$

The quantity of TMA$^+$ delivered to the tissue per second is $Q = In/zF,$ where I is the step increase in current applied to the iontophoresis electrode, n is the transport number, z is the number of charges associated with substance iontophoresed ($+1$ here), and F is Faraday's electrochemical equivalent. The function $erfc$ is the complementary error function. When the experimental medium is agar, by definition, $\alpha = 1 = \lambda$ and $k' = 0$ (Fig. 1), and the parameters n and D are extracted by curve fitting. With knowledge of n and D, the parameters α, λ and k' can be obtained when the experiment is repeated in the brain.

Immunocytochemistry

Following the diffusion measurements, the anesthetized animals were perfused with 4% paraformaldehyde in 0.1 M phosphate-buffered saline (PBS; pH 7.5). Fixed brains were dissected and immersed in PBS with 30% sucrose. Frozen coronal sections (40 µm) were cut through the areas of interest. Astrocytes were identified using monoclonal antibodies to GFAP (Boehringer-Mannheim, Mannheim, Germany).

Immunostaining for chondroitin-sulfate proteoglycan (CSPG) was done using monoclonal antichondroitin sulfate CS-56 antibody (Sigma Chemical Co., St. Louis, MO). GFAP antibodies were diluted 1:20 and CS-56 antibodies were diluted 1:500 in Dulbecco's "A" PBS solution containing 1% bovine serum albumin (BSA; Sigma) and 0.2% Triton X-100. Following overnight incubation in the primary antibody at 4°C, the floating sections were washed and processed using a biotinylated antimouse secondary antibody and the avidin-biotin peroxidase complex method (Vectastain Elite; Vector, Burlingame, CA). Immune complexes were visualized using 0.05% 3,3′-diaminobenzidine tetrachloride (Sigma) in 0.05M Tris buffer (pH 7.6) and 0.02% H$_2$O$_2$.

Slices were mounted on gelatin-coated glass slides and coverslipped.

Statistical Analysis

All data are expressed as mean ± S.E.M. The statistical significance of data from the wounded and contralateral hemispheres was evaluated by one-way ANOVA. Significance was accepted at $P < 0.05$.

RESULTS
Immunocytochemistry

Our first aim was to identify the microelectrode tracks and the location of the electrodes in gliotic tissue during the diffusion experiments (Fig. 1). The second aim was to compare changes in diffusion parameters to the degree of astrogliosis and CSPG expression. The time course of astrogliosis in our study was in agreement with previous findings (Bignami and Dahl, 1974; Mathewson and Berry, 1985; Lindsay, 1986; Hozumi et al., 1990; Vijayan et al., 1990; Hatten et al., 1991; Norton et al., 1992; Bignami and Dahl, 1995), showing that the level of GFAP in the wounded hemisphere was increased as early as 3 days post-lesion; it was most prominent at 7 days (Fig. 1) and declined at 21 and 35 days. We found a clear increase of GFAP immunoreactivity at a distance of 300–1,000 µm from the site of injury; it was less intense at a distance of 1,500–2,000 µm, and only occasionally hypertrophied astrocytes were found throughout the cortex of both the injured and contralateral hemisperes.

We also found a prominent ipsilateral up-regulation of CSPG (Fig. 2). The intensity of staining was maximal at 3 and 7 dpw; however, at 3 dpw, the area of high CSPG expression was greater (nearly all of the ipsilateral hemisphere) than at 7 dpw (Fig. 2A). At 21 and 35 dpw, the staining intensity declined, and proteoglycan expression was restricted to a thin area of the stab wound (Fig. 2D,H).

Measurements of Diffusion Parameters

ECS volume fraction α, tortuosity λ and nonspecific TMA$^+$-uptake k' have been studied in the cortex of young adult rats previously (Lehmenkühler et al., 1993; Mazel et al., 1998; Voříšek and Syková, 1997). In similarly performed experiments, α in cortical layers III–VI ranged from 0.21 to 0.22, whereas λ ranged from 1.57 to 1.62 (Mazel et al., 1998). In the present study, the average α and λ values recorded from the hemisphere contralateral to the wound at 3, 7, 21, or 35 days after stabbing were not significantly different from those in intact animals (Table 1). In the wounded hemisphere diffusion parameters obtained 300–1,000 µm distant from the wound were already changed at 3 dpw; the values of α and λ were substantially higher
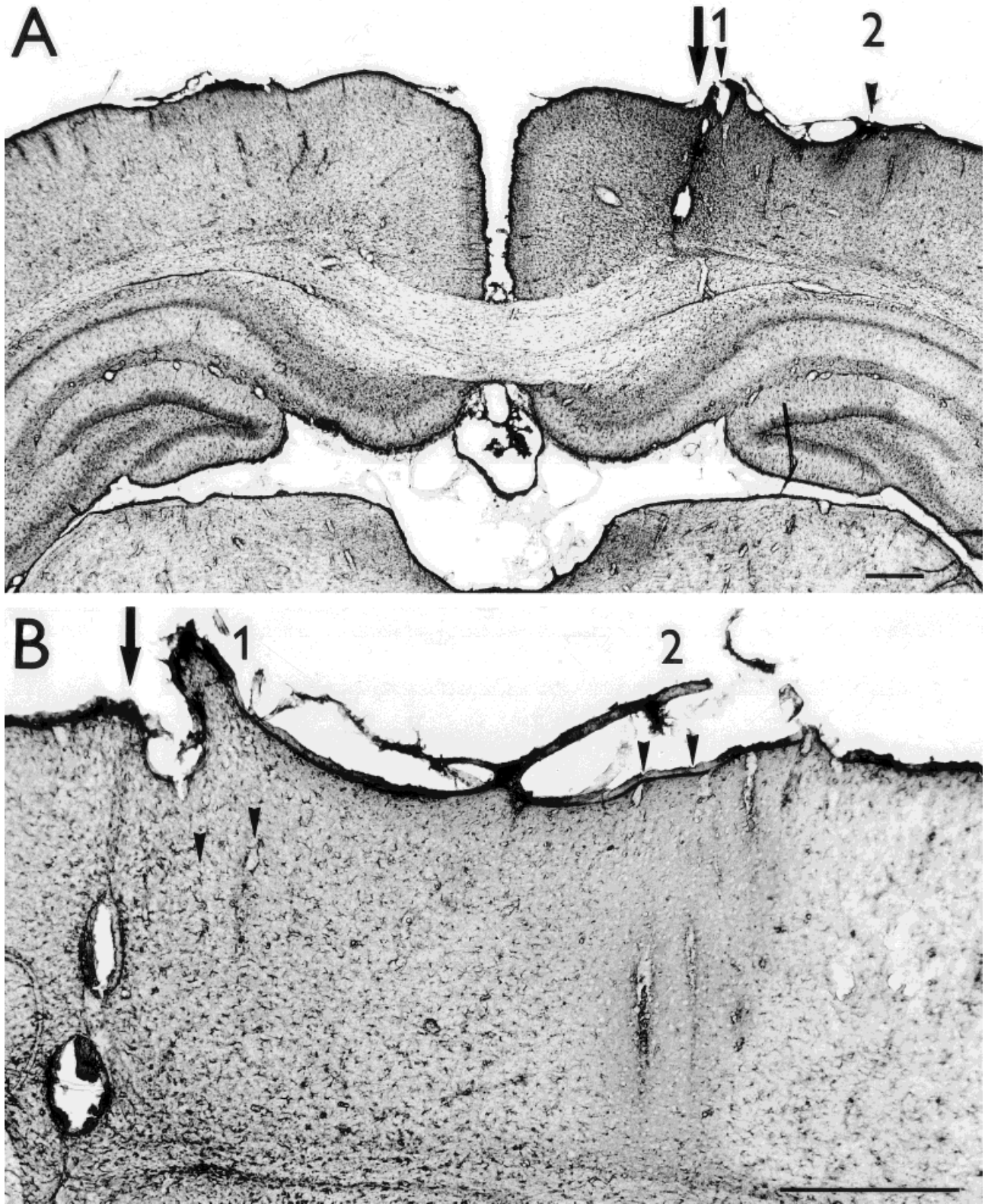
Fig. 1. Reactive astrogliosis in rat cortex immunostained for GFAP 7 days after stabbing. **A:** Coronal section of wounded (right) and contralateral (left) hemispheres after diffusion measurements were performed in the same animal. The arrow points to the stab wound, and the microelectrode tracks are marked by arrowheads for tracks 1 and 2. Note the higher level of GFAP expression in the vicinity of the stab wound. **B:** Wounded hemisphere at higher magnification with arrow pointing to the stab wound and the two identified microelectrode tracks (arrowheads). The microelectrode track 1 (1) passed about 300 µm laterally from the wound, track 2 (2) at about 1,500 µm. Scale bar = 500 µm. For diffusion measurements see Figure 3.
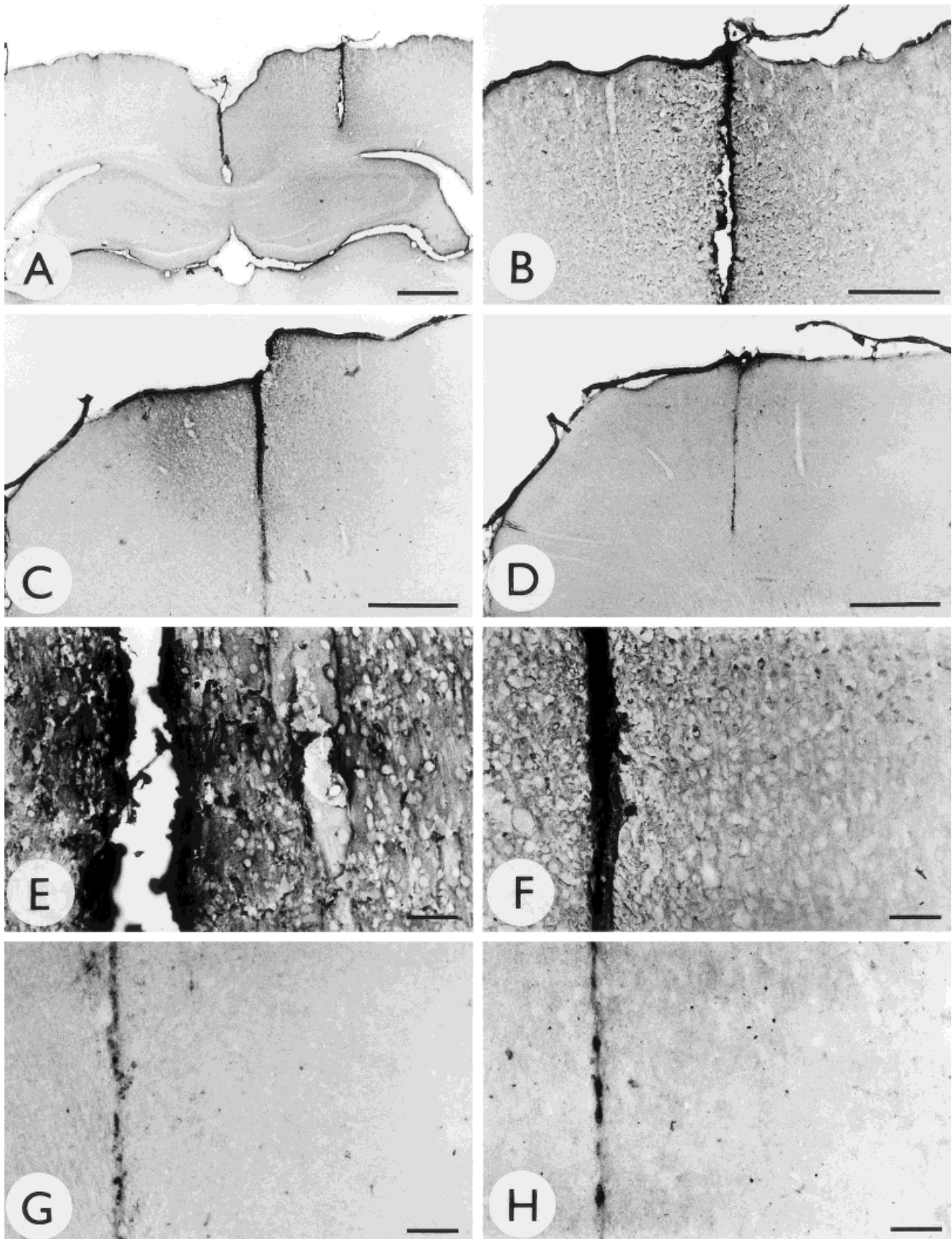
Fig. 2. Photomicrographs showing the changes in CSPG expression at different times after a cortical stab wound. **A:** Coronal section of wounded (right) and contralateral (left) hemispheres of a rat brain at 3 dpw. Note the prominent difference in staining intensity between the two hemispheres. The CSPG immunoreactivity around the wounded site is shown at higher magnification at 3 dpw (**B**), 7 dpw (**C**), and 21 dpw (**D**). Proteoglycan expression decreased from 3 dpw to 7 dpw and at 21 dpw was restricted to a thin area around the wound (D). **E–H:** Views of the tissue at higher magnification in the close vicinity of the stab wound at 3, 7, 21, and 35 dpw, respectively. Scale bars = 1 mm (A), 500 µm (B–D), 100 µm (E–H).

*TABLE 1. Mean values (mean ± S.E.M.) of ECS diffusion parameters in the hemisphere contralateral to the wound and in the wounded hemisphere (SW) at 3, 7, 21, and 35 days after stabbing**

Days after stab wound	Cortical region	N	n	α	λ	$k'\ (\times 10^{-3}\,\mathrm{s}^{-1})$
3	Contralateral h.	10	53	0.21 ± 0.002	1.60 ± 0.008	2.99 ± 0.200
	SW 0.3–1 mm	8	56	0.25 ± 0.005	1.68 ± 0.010	3.04 ± 0.220
				$P < 0.0001$	$P < 0.0001$	
	SW 1.5–2 mm	4	18	0.22 ± 0.008	1.57 ± 0.012	3.39 ± 0.560
7	Contralateral h.	8	54	0.21 ± 0.002	1.61 ± 0.008	3.40 ± 0.290
	SW 0.3–1 mm	9	47	0.26 ± 0.005	1.77 ± 0.013	1.70 ± 0.230
				$P < 0.0001$	$P < 0.0001$	$P < 0.0001$
	SW 1.5–2 mm	4	11	0.22 ± 0.008	1.66 ± 0.014	2.04 ± 0.368
					$P = 0.006$	$P = 0.045$
21	Contralateral h.	7	40	0.22 ± 0.003	1.61 ± 0.010	2.83 ± 0.250
	SW 0.3–1 mm	8	51	0.24 ± 0.005	1.67 ± 0.013	2.05 ± 0.297
				$P = 0.001$	$P < 0.0001$	
	SW 1.5–2 mm	2	8	0.22 ± 0.008	1.65 ± 0.010	2.95 ± 0.460
35	Contralateral h.	2	16	0.21 ± 0.006	1.61 ± 0.018	3.30 ± 0.380
	SW 0.3–1 mm	6	55	0.22 ± 0.003	1.67 ± 0.009	2.39 ± 0.215
					$P = 0.003$	$P = 0.046$
	SW 1.5–2 mm	2	13	0.22 ± 0.003	1.65 ± 0.021	3.38 ± 0.797

*Recordings were made at a distance of either 0.3–1.0 mm or 1.5–2.0 mm laterally from the stab wound. α, ECS volume fraction; λ, ECS tortuosity; k', nonspecific uptake; n, number of measurements; N, number of animals; Contralateral h., hemisphere contralateral to the stab wound; P, the statistical significance of difference vs. contralateral hemisphere. Data are expressed as mean ± S.E.M. from all measured values (n).
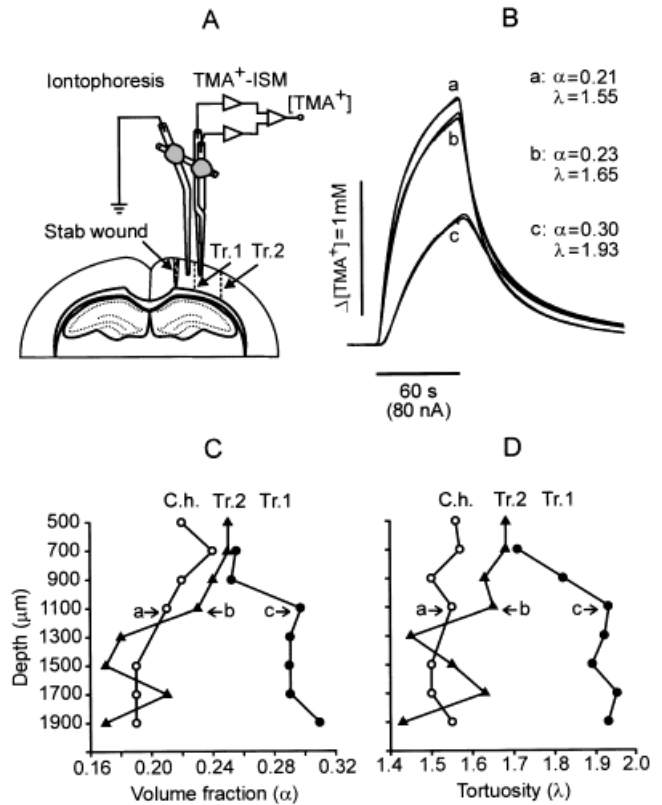

Fig. 3. **A:** Scheme of the experimental arrangement. ECS diffusion parameters were measured by the real-time iontophoretic method using TMA⁺-selective microelectrodes. **B:** Typical examples of TMA⁺ diffusion curves obtained in the contralateral (a) and wounded hemispheres of the same animal at distances of 1,500 μm (b) and 300 μm (c) from the stab wound at a depth of 1,100 μm. The k' values in a, $4.6 \times 10^{-3}\,\mathrm{s}^{-1}$; b, $1.1 \times 10^{-3}\,\mathrm{s}^{-1}$; c, $2.1 \times 10^{-3}\,\mathrm{s}^{-1}$. The concentration scale is linear, and the theoretical diffusion curve is superimposed on each data curve. **C,D:** The graphs show all the values of volume fraction (α) and tortuosity (λ) obtained in the same animal (7 dpw) as shown in Figure 1, in the contralateral hemisphere (C.h., open circles) and in the injured hemisphere during track 1 (Tr 1, solid circles) and track 2 (Tr. 2, triangles). For immunohistochemistry and localization of the tracks, see Figure 1.

than control values. At 7 dpw α and λ reached maximum values, which were significantly higher than those seen at any other time (Table 1, Fig. 3). The values of the diffusion parameters decreased at 21 days but still remained significantly higher than those in the contralateral hemisphere. ECS volume fraction reached control values at 35 dpw, whereas λ remained higher in laminae IV and V (Fig. 4). The mean value of nonspecific cellular uptake $k'\ (10^{-3}\mathrm{s}^{-1})$ at 3 dpw at the wounded site did not differ significantly from that in the contralateral hemisphere (3.04 and 2.99, respectively). It significantly decreased at 7 dpw to a value of 1.70 and remained significantly lower ($k' = 2.39$) than control values ($k' = 3.30$) at 35 dpw (Table 1). The mean values of volume fraction obtained 1,500–2,000 μm distant from the stab wound revealed no significant differences from those obtained in the contralateral hemisphere with the exception of significantly higher values of tortuosity at 7 dpw (Table 1).

After each experiment, microelectrode tracks were identified, and a comparison was made between diffusion parameters and morphological data. A typical example of such analysis is presented in Figures 1 and 3. Figure 1 shows a coronal section of a wounded hemisphere at 7 dpw immunostained for GFAP, with two identified microelectrode tracks. Figure 3 represents the diffusion data from the same experiment showing typical diffusion curves and a graph with the values of α and λ obtained from different depths of the wounded and contralateral hemispheres. The first track passed about 300 μm distant from the wound, i.e., through the regions of high astrocytic reactivity close to the wound (Figs. 1, 3, track 1). The volume fraction increased in astrogliotic tissue to 0.29–0.30 in layers V and VI, tortuosity to values of 1.82 –1.95. This electrode track ended in the corpus callosum in a zone of fibrous astrocytes, also classified as reactive. The values were also large in the corpus callosum: $\alpha = 0.31$ and $\lambda = 1.93$. The second penetration was done further away from the wound, at a distance of 1,500 μm, clearly in an area with lower GFAP reactivity than in the close vicinity of the wound (Fig. 1, track 2). Both diffusion parameters α and λ were lower than in track 1 (Fig. 3). The volume fraction ranged from 0.17 to 0.25, and tortuosity ranged from 1.45 to 1.69. Our data also show that in a single track, located at a greater distance from the wound, where astrogliosis was less pronounced, the mean λ values demonstrate variability, i.e., the ECS diffusion parameters are changed only in some spots and not in others.

Quantile plots of all the α and λ values at a distance of 300–1,000 μm from the wound show larger values at 3, 7, and 21 dpw, compared to those in the contralateral hemisphere (Fig. 5). They also show the greater variabil-
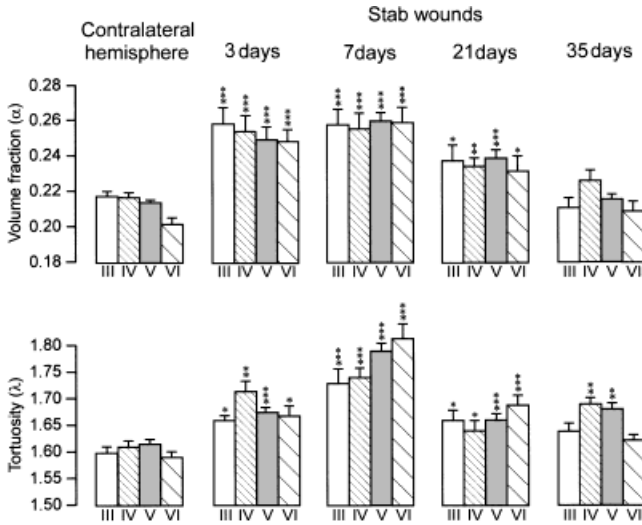
Fig. 4. Graphs showing the means + S.E.M. of all α and λ values obtained in cortical layers III, IV, V, and VI of the wounded hemisphere at 3, 7, 21, and 35 days poststabbing and in the hemisphere contralateral to the wound. Significant differences between the values in injured cortex and the values in the contralateral hemisphere are marked as: ***$P < 0.0001$, **$P < 0.001$, and *$P < 0.05$.
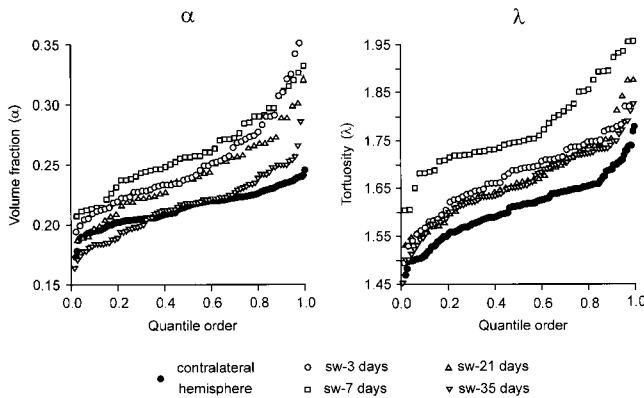

Fig. 5. Quantile plots of all measured α and λ values in the wounded hemisphere at 3, 7, 21, and 35 days after stabbing and in the hemisphere contralateral to the wound. The data for each group were sorted in ascending order, and then each value was plotted against its rank as a fraction of the number of observations in the appropriate group. Note the increase in λ values at 3, 7, 21, and 35 dpw and the similarity of median values of α in the wounded hemisphere and in the contralateral hemisphere at 35 dpw.

ity in individual values in the wounded hemisphere than in the contralateral hemisphere.

The values of α, λ, and k', measured at distances 300 μm and 1,500 μm from the wound at a depth of 1,100 μm (see Fig. 3B, curves b,c), were used to construct isoconcentration circles in the x-y plane (Fig. 6A,B). The constructed circles show the concentration of TMA+ (0.1–1.0 mM) calculated after a 60 s iontophoretic application. The plots illustrate the diffusion pattern and tissue permeation in these two regions of the wounded brain and the differing ability of TMA+ molecules to diffuse in these areas. Figure 6B demonstrates that the neural tissue far from the wound (with
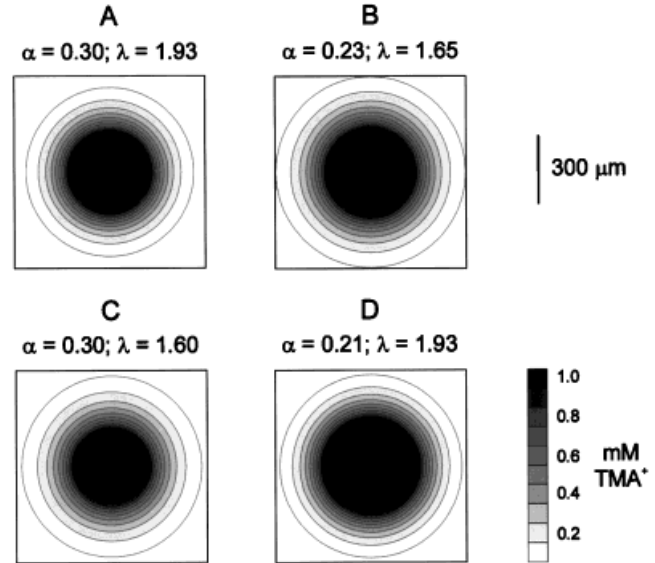

Fig. 6. Two-dimensional isoconcentration plots of TMA+ concentration in two different regions of injured cortex at 7 dpw after a 60 s iontophoretic application of TMA+. **A:** TMA+ concentrations in astrogliotic tissue at a distance of 300 μm from the wound. **B:** TMA+ concentrations at 1,500 μm from the wound, i.e., an area with diffusion parameters approaching those in control animals. Gray densities represent different concentrations of TMA+ from 0.1 to 1.0 mM. Isoconcentration plots were calculated using diffusion parameters obtained from the corresponding diffusion curves b and c shown in Figure 3. k' was in A 2.1×10^{-3} s^{-1} and in B 1.1×10^{-3} s^{-1}. **C** and **D** demonstrate the situation if only α or λ is increased and k' is 1.1×10^{-3} s^{-1}. The iontophoretic pipette served as a point source of TMA+.

less pronounced astrogliosis) is more permissive for diffusing particles such as TMA+ than the severely gliotic tissue close to the wound (Fig. 6A).

DISCUSSION

Our data show severely altered diffusion properties in astrogliotic brain tissue. The study reveals that, the greater the increase in GFAP and CSPG expression, the greater the changes in diffusion parameters. Our data are in agreement with numerous other studies reporting an increase of GFAP immunoreactivity around a wound at 3–4 days after stabbing (Miyake et al., 1988; Hozumi et al., 1990; Norton et al., 1992). The amount of GFAP was maximal at 5–7 days and declined by 21 days (Hozumi et al., 1990; Norton et al., 1992). All previous studies also showed that astrocyte reactivity was more prominent in an approximately 1-mm-wide area around the wound and decreased with distance from the wound, leaving only a relatively thin band of reactive astrocytes surrounding the wound (Mathewson and Berry, 1985).

For the contralateral hemisphere, we only occasionally found reactive astrocytes and no increase in CSPG. Indeed, the volume fraction and tortuosity of the contralateral hemisphere in stabbed animals did not significantly differ from that seen in intact brain in our previous studies (Lehmenkühler et al., 1993; Voříšek

and Syková, 1997). As was reported previously (Moum-djian et al., 1991), contralateral gliosis was observed only after larger and deeper lesions than were used in the current study. The larger extracellular space measured around the wound at 3 days could be caused by the inflammatory reaction and edema in the vicinity of the wound. This can also explain the larger increase in CSPG expression, which quickly spread to a relatively large area of the cortex exceeding the size of the astrogliotic tissue.

Various changes in α and λ have been described in animal models of pathological states. A large ECS volume fraction has been described in the spinal cord of rats with experimental autoimmune encephalomyelitis (EAE) or following X-ray irradiation (Šimonová et al., 1996; Syková et al., 1996). Vasogenic edema, an inflammatory reaction and blood–brain barrier damage in EAE rats result in a dramatic increase in the ECS volume fraction. A significant increase in the ECS volume fraction was also observed in grafted tissue characterized by reactive astrogliosis (Syková et al., 1999a). The increase of ECS volume in the early stages of regeneration after a stab wound may therefore be due to neuronal death, inflammation, and the phagocytic activity of microglia and astrocytes; the subsequent decrease of α at 21 and 35 days can be explained by a second stage of astrocytic response characterized by proliferation and the filling up of the space resulting from the loss of myelin and neurons. The decrease of nonspecific uptake in brain tissue at 7 days after a stab wound can be explained by the fact that reactive astrocytes are mainly switched to other tasks, such as fibrillogenesis (Bignami and Dahl, 1995). In the case of decreased uptake, the neurons could also receive less protection against the toxic effects of excitatory neurotransmitters (Bignami and Dahl, 1995).

Increased tortuosity is a characteristic feature of injured brain tissue. It was also observed in grafted neural tissue that showed severe astrogliosis (Syková et al., 1999a) and in spinal cord when astrogliosis was evoked by a 45 min application of 50 mM K^+ (Syková et al., 1999b). Two possible mechanisms may account for the higher tortuosity. First, astrogliosis is characterized by astrocytic hypertrophy and an increase in the thickness, length, and presumably also number of glial processes, which can form diffusion barriers interposed between the cells. Second, glial cells and brain macrophages produce a variety of macromolecules that could form additional diffusion barriers and increased tissue viscosity. It is generally believed that scar tissue may impede successful regeneration by providing a physical barrier (e.g., proteoglycans, tenascin) to growing neurites (Reier, 1986; Liuzzi and Lasek, 1987; Laywell et al., 1992; Smith-Thomas et al., 1994). Following CNS injury, reactive astrocytes up-regulate various cell surface molecules, including CAMs (Ridet et al., 1997) and extracellular matrix molecules such as laminin and heparan sulphate (Hatten et al., 1991), fibronectin (Egan and Vijayan, 1991), chondroitin-sulfate proteoglycan (Stichel et al., 1995; Ridet et al., 1997; see also Fig.

2), tenascin (Laywell et al., 1992), and keratan sulfate proteoglycan (Geisert et al., 1996). An increased amount and novel types of macromolecules in the CNS may lead to an increase of λ as well as to a greater hindrance to the diffusion of other substances in astrogliotic tissue. Indeed, our preliminary study showed that the application of dextran or hyaluronic acid (HA) solutions resulted in a significant increase of λ in isolated rat spinal cord (Prokopová et al., 1996). The increased expression of ECS matrix molecules may therefore lead to molecular crowding, increased viscosity, and an increase in λ in injured brain tissue (Nicholson and Syková, 1998; Syková, 1997). In this respect, it is also interesting to refer to the study of Levine (1994), who found the maximal expression of chondroitin-sulfate proteoglycan at 7 days after puncture lesions in the rat cerebellum, followed by a decline up to day 35. The transection of the postcommisural fornix resulted in the ipsilateral upregulation of the small chondroitin/dermatan sulfate proteoglycans decorin and biglycan as early as 3 days postlesion; however, the staining patterns of these two proteoglycans were different: Decorin appeared within a wider area around the lesion and preceded the appearance of biglycan (Stichel et al., 1995). Fibronectin immunoreactivity was detected at 2, 3, and 7 days following a penetrating wound through the rat cerebral cortex; the staining pattern at these different times was similar, but the staining intensity at 7 days was much less (Egan and Vijayan, 1991). In our study the increase in CSPG staining was found to be about the same at 3 and 7 dpw, but at 3 dpw the high immunoreactivity was seen in a larger cortical area; a clear decline in staining intensity was observed at 21 and 35 dpw. We therefore suppose that both mechanisms, astrocytic reactivity and an increased amount of macromolecules in the ECS, may affect diffusion in injured tissue and be more important at different times after stabbing.

We conclude that reactive astrogliosis leads to the impairment of diffusion in nervous tissue, owing to the induction of additional diffusion barriers, which may contribute to functional deficits and influence the process of structural and functional regeneration. High tortuosity values will undoubtedly lead to the impaired diffusion of ions, neurotransmitters, trophic factors, and other neuroactive substances in the ECS. A possible explanation for the fact that gliosis in the injured brain contributes to a lack of axonal regeneration (Reier, 1986; Hatten et al., 1991; Geisert et al., 1996) is that the diffusion of large molecules such as growth factors (70 kDa) that support axonal regeneration would be even more hindered than the diffusion of small TMA^+ ions (74 Da). Moreover, the changes in ECS parameters and decreased cellular uptake (e.g., of ions or neurotransmitters) can make injured tissue more susceptible to pathological states, such as anoxia and epilepsia. On the other hand, the reactive astrocytes surrounding the wound may provide a physical barrier limiting the diffusion of toxic agents from the necrotic area to other parts of the brain.

ACKNOWLEDGMENTS

REFERENCES

Agnati LF, Zoli M, Stromberg I, Fuxe K. 1995. Intercellular communication in the brain: wiring versus volume transmission. Neuroscience 69:711–726.

Bignami A, Dahl D. 1974. Astrocyte-specific protein and radial glia in the cerebral cortex of newborn rat. Nature 252:55–56.

Bignami A, Dahl D. 1995. Gliosis. In: Kettenmann H, Ransom BR, editors. Neuroglia. New York: Oxford University Press. p 843–858.

Bjelke B, England R, Nicholson C, Rice ME, Lindberg J, Zoli M, Agnati LF, Fuxe K. 1995. Long distance pathways of diffusion for dextran along fibre bundles in brain: relevance for volume transmission. Neuroreport 6:1005–1009.

Egan RA, Vijayan VK. 1991. Fibronectin immunoreactivity in neural trauma. Brain Res 568:330–334.

Fuxe K, Agnati LF. 1991. Volume transmission in the brain: novel mechanisms for neural transmission. New York: Raven Press.

Geisert EE, Bidanset DJ, Del Mar N, Robson JA. 1996. Up-regulation of a keratan sulfate proteoglycan following cortical injury in neonatal rats. Int J Dev Neurosci 14:257–267.

Hatten ME, Liem RKH, Shelanski ML, Mason CA. 1991. Astroglia in CNS injury. Glia 4:233–243.

Hozumi I, Chiu F-C, Norton WT. 1990. Biochemical and immunocytochemical changes in glial fibrillary acidic protein after stab wounds. Brain Res 524:64–71.

Kullmann DM, Asztely F. 1998. Extrasynaptic glutamate spillover in the hippocampus: evidence and implications. Trends Neurosci 21:8–14.

Laywell ED, Dörries U, Bartsch U, Faissner A, Schachner M, Steindler DA. 1992. Enhanced expression of the developmentally regulated extracellular matrix molecule tenascin following adult brain injury. Proc Natl Acad Sci USA 89:2634–2638.

Lehmenkühler A, Syková E, Svoboda J, Zilles K, Nicholson C. 1993. Extracellular space parameters in the rat neocortex and subcortical white matter during postnatal development determined by diffusion analysis. Neuroscience 55:339–351.

Levine J. 1994. Increased expression of the NG2 chondroitin-sulfate proteoglycan after brain injury. J Neurosci 14:4716–4730.

Lindsay RM. 1986. Reactive gliosis. In: Fedoroff S, Vernadakis A, editors. Astrocytes. Cell biology and pathology of astrocytes. Orlando: Academic Press. p 231–262.

Liuzzi F, Lasek R. 1987. Astrocytes block axonal regeneration in mammals by activating the physiological stop pathway. Science 237:642–645.

Mathewson AJ, Berry M. 1985. Observations on the astrocyte response to a cerebral stab wound in adult rats. Brain Res 327:61–69.

Mazel T, Šimonová Z, Syková E. 1998. Diffusion heterogeneity and anisotropy in rat hippocampus. Neuroreport 9:1299–1304.

Miyake T, Hattori T, Fukuda M, Kitamura T, Fujita S. 1988. Quantitative studies on proliferative changes of reactive astrocytes in mouse cerebral cortex. Brain Res 451:133–138.

Moumdjian RA, Antel JP, Yong VW. 1991. Origin of contralateral reactive gliosis in surgically injured rat cerebral cortex. Brain Res 547:223–228.

Nathaniel EJH, Nathaniel DR. 1981. The reactive astrocyte. In: Fedoroff S, Hertz L, editors. Advances in cellular neurobiology. New York: Academic Press. p 249–301.

Nicholson C, Phillips JM. 1981. Ion diffusion modified by tortuosity and volume fraction in the extracellular microenvironment of the rat cerebellum. J Physiol (London) 321:225–257.

Nicholson C, Syková E. 1998. Extracellular space structure revealed by diffusion analysis. Trends Neurosci 21:207–215.

Norton WT, Aquino DA, Hosumi I, Chiu FC, Brosnan CF. 1992. Quantitative aspects of reactive gliosis: a review. Neurochem Res 17:877–885.

Prokopová S, Nicholson C, Syková E. 1996. The effect of 40-kDa or 70-kDa dextran and hyaluronic acid solution on extracelluar space tortuosity in isolated rat spinal cord. Physiol Res 45:P28.

Reier PJ. 1986. Gliosis following CNS injury: the anatomy of astrocytic scars and their influences on axonal elongation. In: Fedoroff S, Vernadakis A, editors. Astrocytes: cell biology and pathology of astrocytes. Orlando: Academic Press. p 263–324.

Ridet JI, Malhotra SK, Privat A, Gage FH. 1997. Reactive astrocytes: cellular and molecular cues to biological function. Trends Neurosci 20:570–577.

Šimonová Z, Svoboda J, Orkand P, Bernard CCA, Lassmann H, Syková E. 1996. Changes of extracellular space volume and tortuosity in the spinal cord of Lewis rats with experimental autoimmune encephalomyelitis. Physiol Res 45:11–22.

Smith-Thomas L, Fok-Seang J, Stevens J, Du J, Muir E, Faissner A, Geller H, Rogers J, Fawcett J. 1994. An inhibitor of neurite outgrowth produced by astrocytes. J Cell Sci 107:1687–1695.

Stichel CC, Kappler J, Junghans U, Koops A, Kresse H, Muller HW. 1995. Differential expression of the small chondroitin/dermatan sulfate proteoglycans decorin and biglycan after injury of the adult rat brain. Brain Res 704:263–274.

Syková E. 1992. Ionic and volume changes in the microenvironment of nerve and receptor cells. Heidelberg: Springer-Verlag. 167 p.

Syková E. 1997. The extracellular space in the CNS: Its regulation, volume and geometry in normal and pathological neuronal function. Neuroscientist 3:28–41.

Syková E, Roitbak T, Mazel T, Šimonová Z, Harvey AR. 1999a. Astrocytes, oligodendroglia, extracellular space volume and geometry in rat fetal brain grafts. J Neurosci 91:783–798.

Syková E, Svoboda J, Polák J, Chvátal A. 1994. Extracellular volume fraction and diffusion characteristics during progressive ischemia and terminal anoxia in the spinal cord of the rat. J Cereb Blood Flow Metab 14:301–311.

Syková E, Svoboda J, Šimonová Z, Lehmenkühler A, Lassmann H. 1996. X-irradiation-induced changes in the diffusion parameters of the developing rat brain. Neuroscience 70:597–612.

Syková E, Vargová L, Prokopová S, Šimonová Z. 1999b. Glial swelling and astrogliosis produce diffusion barriers in the rat spinal cord. Glia 25:56–70.

Vijayan VK, Lee YL, Eng LF. 1990. Increase in glial fibrillary acidic protein following neural trauma. Mol Chem Neuropathol 13:107–118.

Voříšek I, Syková E. 1997. Evolution of anisotropic diffusion in the developing rat corpus callosum. J Neurophysiol 78:912–919.

Zoli M, Jansson A, Syková E, Agnati LF, Fuxe K. 1999. Intercellular communication in the central nervous system. The emergence of the volume transmission concept and its relevance for neuropsychopharmacology. Trends Pharmacol Sci 20:142–150.